



**HAL**  
open science

## Observing ice clouds in the submillimeter spectral range: the CloudIce mission proposal for ESA's Earth Explorer 8

S. Buehler, E. Defer, F. Evans, S. Eliasson, J. Mendrok, P. Eriksson, C. Lee, C. Jiménez, C. Prigent, S. Crewell, et al.

### ► To cite this version:

S. Buehler, E. Defer, F. Evans, S. Eliasson, J. Mendrok, et al.. Observing ice clouds in the submillimeter spectral range: the CloudIce mission proposal for ESA's Earth Explorer 8. *Atmospheric Measurement Techniques*, 2012, 5 (7), pp.1529-1549. 10.5194/amt-5-1529-2012 . hal-02867541

**HAL Id: hal-02867541**

**<https://hal.science/hal-02867541>**

Submitted on 15 Jan 2021

**HAL** is a multi-disciplinary open access archive for the deposit and dissemination of scientific research documents, whether they are published or not. The documents may come from teaching and research institutions in France or abroad, or from public or private research centers.

L'archive ouverte pluridisciplinaire **HAL**, est destinée au dépôt et à la diffusion de documents scientifiques de niveau recherche, publiés ou non, émanant des établissements d'enseignement et de recherche français ou étrangers, des laboratoires publics ou privés.



Distributed under a Creative Commons Attribution - NonCommercial 4.0 International License



## A new disjunct eddy-covariance system for BVOC flux measurements – validation on CO<sub>2</sub> and H<sub>2</sub>O fluxes

R. Baghi<sup>1</sup>, P. Durand<sup>1</sup>, C. Jambert<sup>1</sup>, C. Jarnot<sup>1</sup>, C. Delon<sup>1</sup>, D. Serça<sup>1</sup>, N. Striebig<sup>2</sup>, M. Ferlicoq<sup>3</sup>, and P. Keravec<sup>3</sup>

<sup>1</sup>Laboratoire d'Aérodynamique, UMR5560, CNRS – Université de Toulouse and Centre National de la Recherche Scientifique, Toulouse, France

<sup>2</sup>Observatoire Midi-Pyrénées, Toulouse, France

<sup>3</sup>Centres d'Etudes Spatiales de la Biosphère (CESBIO), UMR5126, Toulouse, France

Correspondence to: R. Baghi (romain.baghi@aero.obs-mip.fr)

Received: 9 May 2012 – Published in Atmos. Meas. Tech. Discuss.: 13 June 2012

Revised: 16 November 2012 – Accepted: 28 November 2012 – Published: 21 December 2012

**Abstract.** The disjunct eddy covariance (DEC) method is an interesting alternative to the conventional eddy covariance (EC) method because it allows the estimation of turbulent fluxes of species for which fast sensors are not available. We have developed and validated a new disjunct sampling system (called MEDEE). This system is built with chemically inert materials. Air samples are taken quickly and alternately in two cylindrical reservoirs, the internal pressures of which are regulated by a moving piston. The MEDEE system was designed to be operated either on the ground or aboard an aircraft. It is also compatible with most analysers since it transfers the air samples at a regulated pressure. To validate the system, DEC and EC measurements of CO<sub>2</sub> and latent heat fluxes were performed concurrently during a field campaign. EC fluxes were first compared to simulated DEC (SDEC) fluxes and then to actual DEC fluxes.

Both the simulated and actual DEC fluxes showed a good agreement with EC fluxes in terms of correlation. The determination coefficients ( $R^2$ ) were 0.93 and 0.91 for DEC and SDEC latent heat fluxes, respectively. For DEC and SDEC CO<sub>2</sub> fluxes  $R^2$  was 0.69 in both cases. The conditions of low fluxes experienced during the campaign impaired the comparison of the different techniques especially for CO<sub>2</sub> flux measurements. Linear regression analysis showed an 14 % underestimation of DEC fluxes for both CO<sub>2</sub> and latent heat compared to EC fluxes.

A first field campaign, focusing on biogenic volatile organic compound (BVOC) emissions, was carried out to measure isoprene fluxes above a downy oak (*Quercus Pubescens*) forest in the south-east of France. The measured standard

emission rate was in the lower range of reported values in earlier studies. Further analysis will be conducted through ground-based and airborne campaigns in the coming years.

### 1 Introduction

Chemistry in the lower atmosphere is mostly driven by sources and sinks of trace species at the Earth's surface. Reciprocally, the biosphere is affected by changes in atmospheric properties (Pielke et al., 1998). Flux measurements are essential for quantifying atmosphere–biosphere exchanges and understanding physical and chemical processes in the atmosphere but they are often difficult to obtain. There are two widely used groups of flux measurement techniques: enclosure and micrometeorological techniques.

Enclosure techniques can be relatively inexpensive and used over ground, water, or vegetation. Enclosures allow emission rates of the enclosed subject to be monitored by using various analysers (gas chromatography coupled to a mass spectrometer, to a flame ionization detector or other analysers). For static enclosures, fluxes are obtained by following the evolution of concentrations in the enclosure. In dynamic chambers, mostly used for BVOC fluxes, a steady-state flow of air is passing through the enclosure. However, in most cases, the measurements are representative of a very small area and can disturb the enclosed environment (Dabberdt et al., 1993).

Micrometeorological techniques consist of measuring the vertical turbulent flux near the surface. They provide

integrated fluxes over, e.g., crop fields or forest canopies. Among these micrometeorological techniques, eddy covariance (EC) is the most direct method for estimating surface-atmosphere exchanges (Baldocchi et al., 1988; Aubinet et al., 1999). It relies on measuring both vertical velocity ( $w$ ) and scalar-of-interest concentration ( $c$ ) at a high rate to characterize the vertical mass flux carried by eddies of all sizes. The flux is then estimated from the covariance of  $w$  and  $c$  fluctuations averaged over a period of time. The averaging period must be long enough to be statistically representative but short enough to meet the assumption of steady state conditions. EC measurements of BVOC fluxes are not always possible due to instrumental limitations. Instruments with short enough response time are available but do not provide continuous time series for multiple VOC flux measurements or require longer analysis time to achieve sufficient sensitivity. Alternative approaches allowing longer analysis time have been proposed to extend the use of micrometeorological flux methods. For fairly short-lived species, the turbulent flux provided by micrometeorological techniques is similar to the surface flux as long as the measurement height is only a few metres above the surface, otherwise chemical reactions occur and affect the flux (Kristensen et al., 2009).

The gradient method is used as an alternative to EC and relies on surface layer similarity theory (flux-profile relationships). It consists of measuring mean concentrations at different heights in the surface layer. The flux is then estimated from the concentration profile, the stability parameter (Obukhov length) and friction velocity. This method is indirect since it requires an empirical parameterization. Furthermore, when the chemical reaction time is not much longer than the turbulent diffusion characteristic time, the impact of chemistry on profiles has to be taken into account through a coupled chemistry-dynamics model (Kristensen et al., 2009).

The eddy accumulation (EA) method initially proposed by Desjardins (1977) was aimed at increasing sample analysis time but was a technical challenge. With this method, air is sampled in two separate reservoirs depending on the sign of the vertical wind velocity. The sampling rate has to be proportional to the vertical velocity, which is very difficult to achieve. Businger and Oncley (1990) simplified the EA technique by introducing an empirical calibration and named this method relaxed eddy accumulation (REA). The REA method requires samples to be collected in separate downdraft and updraft reservoirs as with the EA method, but with a constant flow. The flux is then proportional to the product of (1) the concentration difference between the two reservoirs over the same period as for the EC technique (e.g., 30 min), (2) the standard deviation of  $w$ , with a scaling coefficient  $\beta$ , which is dependent upon the statistical properties of the time series and the  $w$  threshold values above which the air is collected (Businger and Oncley, 1990; Andreas et al., 1998; Fotiadis et al., 2005). While the REA method is relatively easy to implement in the field, it cannot be used for species whose

characteristic reaction time is not much longer than the accumulation period.

Finally, the disjunct eddy covariance method (DEC) is derived from EC, and differs only by the number of samples captured. This method allows a sampling rate as low as one sample every  $\sim 10$ – $30$  s, whereas data are acquired at a high rate for EC measurements (10–20 Hz) (Rinne et al., 2001). Among alternative techniques of EC, the DEC approach is the only one that does not rely on any parameterization and does not involve further assumptions. However, air samples must be acquired in a very short time (a few tenths of a second at most) and precisely dated to capture the turbulent transport (Rinne et al., 2001; Turnipseed et al., 2009). When fluxes of reactive compounds are to be measured, characteristic chemical time scales have to be longer than (or at least comparable to) turbulent transport time scales (Vila-Guerau de Arellano and Duynkerke, 1992). Flux measurements of short-lived species are an issue when using EC alternative techniques as they often require intermediate storage of samples before analysis. Thus, the DEC method offers an advantage with a storage time that is two orders of magnitude lower than that required for the REA technique. Advances in the technology of proton transfer reaction mass spectrometry (PTR-MS) (Blake et al., 2011), a fast response analyser capable of sequentially measuring a wide array of organic compounds present in our atmosphere, have extended the range of species whose flux can be measured with the EC or DEC technique. A variant of DEC, named virtual DEC (VDEC), was specifically designed for the PTR-MS instrument (Karl et al., 2002). With this method, it is possible to achieve flux measurements of several trace gases simultaneously, without the use of intermediate reservoirs and using only one PTR-MS instrument.

Several disjunct eddy samplers (DES) are described in the literature (Rinne et al., 2000, 2008; Grabmer et al., 2004; Turnipseed et al., 2009). For biogenic emission measurements these DESs have been used with either an infra-red gas analyser (IRGA) or PTR-MS. Some of them present limitations: Rinne et al. (2008) demonstrated the validity of the DEC technique through direct comparison between DEC and EC latent heat flux but, in their DES, the air was re-injected into the reservoirs once it had been analyzed by the IRGA, in order to avoid a pressure drop during the analyses. Such a system is only suitable for certain analysers which neither destroy nor contaminate the sample during the analysis.

In this study, we present the design of an innovative disjunct eddy sampler named MEDEE for tower-based and airborne DEC measurements. MEDEE stands for “Mesure par Échantillonnage Disjoint des Échanges d’Espèces en trace” (trace gas exchange measurements by disjunct sampling). Our primary objective in developing this instrument was to measure biogenic VOC (BVOC) fluxes but the design of MEDEE offers compatibility with a wide range of compounds and analysers. As mentioned above, the DEC method has many advantages over other

micrometeorological techniques for compounds for which fast response analysers are not available.

The paper is organized as follows: in Sect. 2, a brief theoretical background of EC and DEC techniques is given. Then we describe the MEDEE instrument in detail (Sect. 3). In Sect. 4, we report the results from a field campaign set up for the validation of the MEDEE system. Latent heat and CO<sub>2</sub> fluxes were measured concurrently by MEDEE coupled to a closed path IRGA, and by the EC technique, over a winter wheat plot during summer 2011. Finally, the results from a field test campaign focused on BVOC emissions are reported in Sect. 5.

## 2 Theoretical background

### 2.1 Eddy covariance method

Trace gases and energy are transported between the Earth's surface and the atmosphere via turbulent upward and downward motions in the air. In the eddy covariance technique, fast rate monitoring of these turbulent motions allow the net exchange between the surface and the atmosphere to be determined. The vertical flux of a scalar in the turbulent layer above the surface is described as the mean product of the vertical wind component  $w$  and the scalar concentration  $c$ :

$$F = \overline{wc}. \quad (1)$$

Equation (1) requires the time series of  $w$  and  $c$  to be quantified at a rate and over a duration that allows sampling of all the scales that contribute to the covariance (i.e. the scales at which the  $(w, c)$  cospectrum is significant). In general, a 10–20 Hz sampling frequency over a 20–30 min period of time is adequate for surface flux estimates. Equation (1) is solved using Reynolds decomposition of  $w$  and  $c$  into their mean and fluctuation values. Considering that  $\overline{w}$  is non-zero (even over flat, homogeneous terrain) when a buoyancy flux exists (Webb et al., 1980; Foken and Wichura, 1996), there are two ways to estimate  $F$  from the fluctuations of  $w$  and the scalar concentration. The first way is to compute  $F$  from the covariance  $\overline{w'c'}$  and to correct the value according to the buoyancy flux (the so-called “Webb correction”, see e.g., Webb et al., 1980; Fuehrer and Friehe, 2002; Lee and Massman, 2011). The second way is to compute the covariance between  $w'$  and the scalar mixing ratio relative to dry air  $\chi'$ .  $F$  is thus estimated as

$$F = \rho_a \overline{w'\chi'}, \quad (2)$$

where  $\rho_a$  is the mean density of dry air.

### 2.2 Disjunct eddy covariance method

DEC was derived from EC as a means of using slower analysers. The vertical wind is measured at high rate but, unlike in the EC method, samples are separated by a constant time

interval  $\Delta t$ . Samples are captured quickly (e.g. in 0.2 s) and analyzed until the next sample is taken. The turbulent flux is thus determined as the average covariance of the available number  $n$  of discrete samples over the flux calculation period:

$$F = \rho_a \frac{1}{n} \sum_{i=1}^n (w'\chi')_i. \quad (3)$$

It has been shown that, as long as the time interval  $\Delta t$  between two measurements is not much longer than the integral time scale of the turbulence, the flux can be estimated with only a small increase in random error (Lenschow et al., 1994). The number of samples  $n$  depends on  $\Delta t$ , which is generally between 1 s and 30 s. On the other hand, when the sampling interval is longer than the integral time scale, the samples can be assumed to be statistically independent. In such conditions, Rinne et al. (2002, 2008) used two ways to estimate the uncertainty on the DEC flux (random error) according to the number of measurements available for an averaging period of half an hour (Fig. 1). If  $N$  is the number of points of the full high-rate EC time series, and  $n$  the number of points of the sub-sample, then a theoretical estimate of the uncertainty of the covariance computed on the  $n$ -values is given by (Rinne et al., 2008):

$$\varepsilon_{w'\chi'} = \sqrt{\frac{(w'\chi')^2}{n} \frac{N-n}{N-1}} \approx \frac{\sigma_{w'\chi'}}{\sqrt{n}}, \quad \text{if } N \gg n. \quad (4)$$

In the above equation,  $\sigma_{w'\chi'}$  is the standard deviation of the  $w'\chi'$  time series. The error  $\varepsilon_{w'\chi'}$ , normalized by  $\sigma_{w'\chi'}$ , is represented by the continuous line in Fig. 1. The uncertainty can also be estimated by taking measured high-rate time series, generating sub-sampled (at a lower rate) time series from them and computing the corresponding covariances. The standard deviation of the covariance values for a given number of disjunct samples  $n$  gives an estimate of  $\varepsilon_{w'\chi'}$ . Rinne et al. (2002, 2008) and Rinne and Ammann (2012) reported the results of such simulations on ground and airborne measurements. In Fig. 1 we reproduce their results obtained with observations above an alfalfa field (Rinne et al., 2008). The uncertainty simulated by Eq. (4) follows the behavior of the data points well, with a small overestimation. This figure illustrates that, as long as  $n$  is of the order of or larger than  $\sim 100$ , the statistical uncertainty on the covariance estimate remains acceptable.

As mentioned above, the use of Eq. (4) is restricted to data for which the integral time scale of  $w'\chi'$  is shorter than the sample time interval. Estimates of these integral scales in the atmospheric surface layer are very scarce. In Lohou et al. (2010), the mean of the integral length scale of  $w'q'$  is estimated to be 4–5 m ( $\pm 3$  m standard deviation) in the surface layer above a western African wet savannah. From these values we can estimate that the integral time scale is below 10 s as long as the mean wind speed is higher than  $0.5 \text{ m s}^{-1}$

(i.e. most of the time). This implies that, with a time interval of 11.5 s (the value used in the experiment described later on) we can assume our samples to be statistically independent and use Eq. (4) to estimate uncertainty. The arrow on Fig. 1 indicates the number of samples of the MEDEE system during the two field campaigns of the present study. The expected uncertainty normalized by the standard deviation of the  $w'\chi'$  time series is thus no larger than 8%.

Sample carry over is an additional source of uncertainty and bias (Langford et al., 2009). It results from the air remaining in the reservoir because of the partial vacuum before the capture of the next sample, and from the air remaining in the “dead volume” between the reservoir and the on-line analyser. The period of time required to fill the reservoirs should also be considered as a source of uncertainty. The filling time is in general longer than the vertical wind measurement rate ( $\sim 0.1$  s), which acts as a filter for higher frequencies. The consequences of these two error sources will be analyzed in the following sections.

### 3 Disjunct eddy sampler

MEDEE was designed to be operated on the ground as well as aboard a plane. It was built to fit into a 19" rack. Sampling parts are mounted on a sturdy anodized aluminium plate and electronic modules are embedded in several rack compartments. MEDEE was developed to collect a small air sample promptly (at  $\sim 0.2$  s), and to ensure its transfer at a constant regulated pressure to an on-line gas analyser. This is new and has not been reported before. It enables the use of pressure sensitive analysers pumping in a closed reservoir. A scheme of the MEDEE system is shown in Fig. 2.

MEDEE comprises two stainless-steel cylindrical reservoirs. Each cylinder is connected to a stainless-steel piston moved by an electric actuator, thus making volumes variable. This technology allows real-time compensation of any pressure drop in the reservoirs. Airtightness is ensured by Teflon seals and Teflon guides prevent the pistons from misalignment. Each cylinder is connected to the fluid circuit and to a pressure transducer (A-10, WIKA Instruments, Cergy Pontoise, France) for pressure measurement within the cylinder. The cylinders are 130 mm long with an inner diameter of 100 mm, which corresponds to a maximum volume of 1 L. High flow conductance solenoid valves (72B11DCM, Peter Paul Electronics, New Britain, CT, USA) with stainless-steel bodies serve as sample inlets. Teflon bodied solenoid valves (Type 121, Burkert, Ingelfingen, Germany) are used to direct the flow towards the analyser or towards a vacuum pump (80110131, Thomas, Wayne, PA, USA). All solenoid valves have a fast response time ( $< 50$  ms). Stainless-steel connectors and Teflon pipes (9.6 mm inner diameter) are used to connect the cylinders to sample inlets, while 4-mm-inner-diameter Teflon pipes are used for the analyser and vacuum circuits. To reduce the errors resulting from sensor separa-

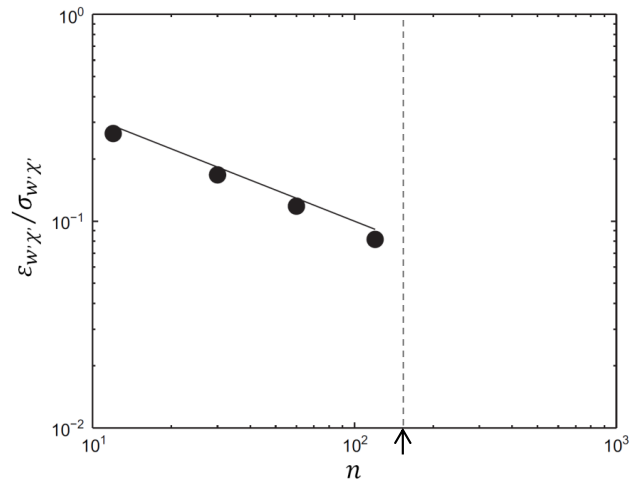


**Fig. 1.** Evolution of the accuracy of the DEC flux estimate according to the number of values over the averaging period. The solid line is the theoretical flux uncertainty according to Eq. (4). The filled circles represent the uncertainties on DEC fluxes simulated from sub-sets of 12, 30, 60 and 120 samples. The dotted line indicates the number of samples produced by MEDEE with a sample capture every 11.5 s. Reproduced and adapted from Rinne et al. (2008).

tion (Moore, 1986), the inlet solenoid valves are moved to be as close as possible to the wind measurement point, which increases the reservoir volume while minimizing the capture lag time with respect to the vertical wind measurement. For the validation field campaign described below, the total reservoir volume was thus extended to 1.78 L. In the same way, on the line towards the analyser, the solenoid valves could be placed in such a position that the dead volume before the analyser would be minimum.

This sampling system can be represented as two mechanical syringes. A 3-D model of one mechanical syringe is depicted in Fig. 3. The reservoir walls have been made transparent to reveal the piston. Teflon bellows hermetically seal the connection between the electric actuator arm and the piston, and prevent grease degassing.

MEDEE is operated by a LabVIEW (National Instruments) program running on an embedded box PC, and a micro-controller chip that gives the rhythm of the operating phases and triggers the solenoid valves. A servomechanism implemented in the program drives the piston through the electric actuator according to the pressure value inside the reservoir. Pressure values and on-line gas analyser data are stored on a data-logger (CR1000, Campbell Scientific Inc., Logan, UT, USA), the former at a rate of 20 Hz and the latter at 10 Hz. Extra entries available on this data acquisition system are used for sonic anemometer data storage if the system is operated on the ground or synchronization parameters if the system is on board the aircraft.

The two “mechanical syringes” work alternately. With respect to a single system, this can double the number of

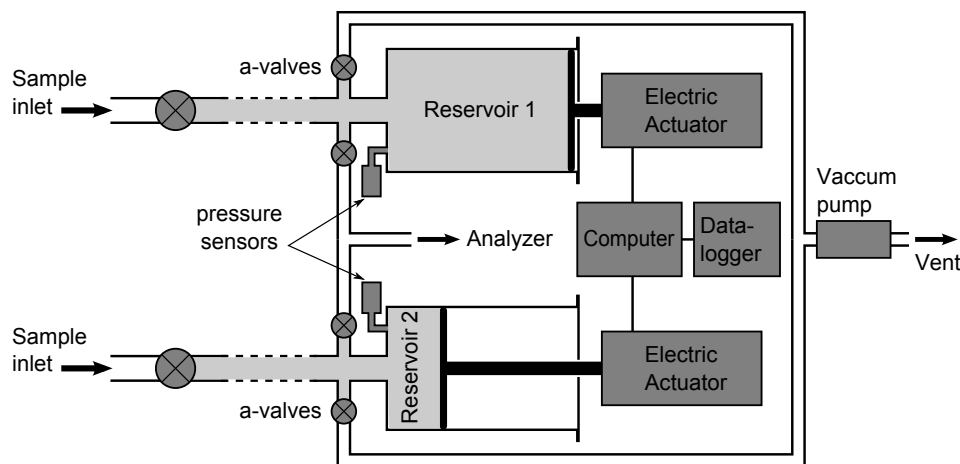


Fig. 2. Scheme of the MEDEE system.



Fig. 3. 3-D drawing of one of the two “mechanical syringes” of the MEDEE system. The cylindrical reservoir is made transparent on the illustration in order to show the moving piston. The gray rectangular box on the left houses the jack screw, which is moved by the engine inside the black compartment above it.

samples and continuously feeds air samples to the analyser. A full cycle of operation for one system is divided into three main phases: (1) establishing the vacuum, (2) sampling, and (3) transferring to the analyser at a constant regulated pressure (see Fig. 4). During the first step, the reservoir pressure is brought down to  $\sim 20\text{--}40\text{ hPa}$  with a vacuum pump and by pulling down the piston in the cylinder forward and backward. The sample grab is then triggered by opening the inlet valve. Once captured, the sample is transferred to the analyser by opening the analysis valve. At the end of this sequence, the second reservoir is ready to transfer a new sample. The synchronization between the valves on the two reservoirs allows the analyser to receive samples following one another without interruption.

The pressure regulation is ensured by the electric actuator in response to the measured pressure in the reservoir. The set

point pressure used for the regulation is the value measured in the reservoir when the instrument is in starting phase (all valves open), and thus corresponds to the atmospheric pressure at this time. This regulation allows the analyser to draw sample air without experiencing a pressure drop that would disturb the flow rate and analyser response. Pressure cycles inside the reservoirs are illustrated in Fig. 5. The three main phases of operation are emptying, sampling, and analysing. The figure highlights the low-pressure level reached at the end of the emptying phase, and the pressure regulation during the analysis periods, marked by the horizontal arrows. Given that the pressure signal resolution is not better than 1 hPa, we observe a fairly stable value ( $\pm 2\text{ hPa}$ ), at least during the last  $\sim 70\%$  of the analysis period. In the switching periods and during the beginning of the analysis, the pressure fluctuations are somewhat higher but remain within  $\pm 5\text{ hPa}$ . Before the capture, the pressure is no higher than 40 hPa, which limits the contamination of the sample by air remaining from the previous one.

In the cycle shown on Fig. 4, 11.5 s are dedicated to the analysis of an air sample. This is also the time interval  $\Delta t$  between two consecutive samples. This value can be adjusted between 10 and 30 s with this instrument. For a  $\Delta t$  of 11.5 s, 155 samples are analyzed in half an hour, which would correspond to a low uncertainty on the covariance estimate (see Fig. 1).

When MEDEE is switched on, a pre-loading phase starts. Inlet solenoid valves are opened to equilibrate reservoirs to ambient pressure, followed by the opening of analysis valves allowing air to flow freely from the inlet to the analyser. In this standby configuration, the analyser can be turned on for pre-heating. Next, a manual switch triggers the disjunct sampling sequence. A first reservoir is emptied before sampling while air is flowing to the analyser through the second reservoir, and the operational cycle starts with the first capture.

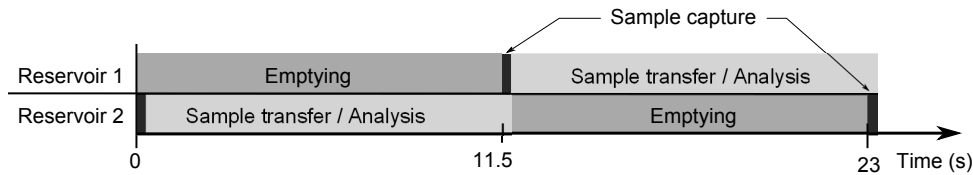


**Fig. 4.** The three steps of the MEDEE operating cycle (emptying, capture and analysis), for each of the two reservoirs.

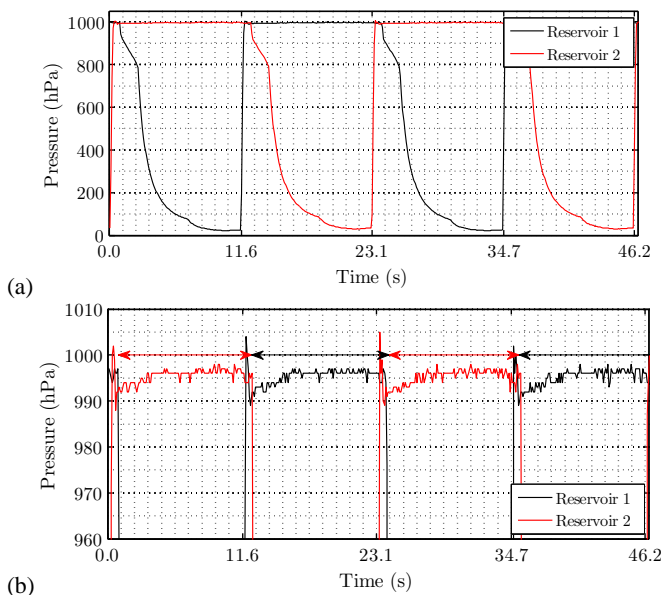


**Fig. 5.** (a) Pressure (hPa) cycles inside MEDEE's reservoirs displayed full scale. (b) The bottom diagram is identical but the pressure scale is zoomed around atmospheric value (here 996 hPa). The red and black signals correspond to the two reservoirs. The horizontal arrows indicate the analysis periods of each sample. Pressure peaks of some hPa are observed at the end of the captures but the analyses start later on.

When stopped, MEDEE returns to a standby mode similar to the one at the beginning. The current analysis is completed and both inlet valves are opened to the ambient air. The second analysis valve is then opened and the air can flow freely to the analyser. The system can be run for several days without interruption.

## 4 Validation campaign

### 4.1 Site description

A field campaign was carried out from 9 June to 17 June 2011 on a site located at Lamasquère, a country area 12 km from Toulouse (south-west France). The Lamasquère site is characterized by a cultivated plot of 0.32 km<sup>2</sup> on flat terrain. It is part of the Carbo-Europe network (Dolman et al., 2006) and

has been instrumented for meteorological and micrometeorological measurements since March 2005. CO<sub>2</sub> and water vapour fluxes are monitored continuously at the site. The altitude is 180 m, and the mean annual wind speed is 1.79 m s<sup>-1</sup>. Main wind directions are from the west and east-south-east with a fetch of 200 and 140 m, respectively. Crop management consists of rotation of winter wheat and maize. An exhaustive description of the field site is given in Béziat et al. (2009). During the validation campaign, CO<sub>2</sub> and water vapour turbulent flux measurements were performed concurrently by the conventional EC method and the DEC method over a senescent winter wheat (*Triticum aestivum*) crop. The instruments were installed in the middle of the plot for an optimal fetch along the main wind directions. The average air temperature during the measurement period was 18.5 °C. The hottest day was 15 June with a maximum of 29 °C reached during the early afternoon. Weather conditions were mostly sunny, but 10 and 16 June were cloudy with some short rain events. The experiment took place during the ripening stage of the winter wheat when plants had become photosynthetically less active and were drying. CO<sub>2</sub> uptake and plant transpiration were thus expected to be low. The crop was harvested on 2 July, two weeks after the end of this experiment.

### 4.2 Eddy covariance measurements

The eddy covariance instrumentation set up was composed of a three-dimensional sonic anemometer (CSAT 3, Campbell Scientific Inc, Logan, UT, USA) for wind components and speed of sound (from which the “sonic” temperature was deduced), and an open-path infrared gas analyser (LI-7500, LI-COR, Lincoln, NE, USA) for CO<sub>2</sub> and water vapour concentrations. Both sensors were installed on a mast at 3.65 m above the ground. Data were recorded with MEDEE's datalogger at 10 Hz. EC fluxes of CO<sub>2</sub> and H<sub>2</sub>O were calculated using MATLAB routines with linear detrending. No density correction on the fluxes (Webb et al., 1980) was needed as concentration measurements were converted to mixing ratios and fluxes were computed according to Eq. (2). H<sub>2</sub>O fluxes were multiplied by the latent heat of vaporisation of water  $L_v$  and thus converted into latent heat flux expressed in W m<sup>-2</sup>.

### 4.3 Disjunct eddy covariance measurements

During this experiment, the same sonic anemometer was used for the EC and DEC measurements. MEDEE was coupled to a closed-path infrared gas analyser (LI-6262, LICOR, Lincoln, NE, USA) for disjunct eddy covariance measurement of CO<sub>2</sub> and water vapour fluxes. Both instruments were installed next to the EC mast. MEDEE's inlet solenoid valves were moved away from the sampling system and brought closer to the wind measurement point (0.2 m). Two-metre long, 9.6-mm-inner-diameter Teflon tubing was used between the inlet valves and the sampling system. The same type of Teflon line 60 cm in length was used as the inlet from the solenoid valves toward the sonic anemometer. In this configuration, the dead volume contained in the tubing upstream of the inlet solenoid valves represented 2.4 % of the reservoir volume (43 mL). Longer tubing slightly impaired the sampling duration, which increased to  $\sim 0.3$  s, during which time the reservoir filling was observed to be almost linear. All sensor signals were stored on MEDEE's data-logger to avoid synchronization issues.

The LI-6262 and the LI-7500 analysers have been calibrated separately before the field measurements. In order to evaluate the difference in calibration between the two analysers, a period of time during the field campaign was dedicated to inter-compare concentration fluctuations. For water vapor fluctuations, the agreement between the two analysers was 99 %, whereas for CO<sub>2</sub> fluctuations the LI-6262 analyser measured values 23 % higher than those of the LI-7500. The concentrations measured by the LI-6262 were therefore adjusted accordingly to compensate for this difference.

DEC flux calculations were done by a MATLAB routine where samples were dated precisely using reservoir-pressure time series. The vertical wind values falling within the reservoir linear filling period were averaged and used with the gas mixing ratio values for the covariance calculation. Gas mixing ratio measurements were averaged over periods of 5 s during the analysis time with rejection of the first 6 seconds, to allow for the stabilization of the pressure in the reservoir and the time for sample transfer from the reservoir to the analyser. EC and DEC fluxes were computed according to Eqs. (2) and (3), respectively.

This study was not intended to provide fluxes for an annual budget but to prove the agreement of the two measurement techniques. Since both techniques used the same wind data, further processing steps (e.g., sonic coordinate rotation) were not needed.

### 4.4 Data quality and processing

The time series of the main parameters measured during half an hour (05:30 to 06:00 UTC on 15 June) are presented in Fig. 6. During this half-hour period, the  $w$  fluctuations did not exceed  $0.5 \text{ m s}^{-1}$  because of the moderate (but increasing) turbulence in the growing boundary layer. CO<sub>2</sub> concen-

tration started at 600 ppm, resulting from nighttime accumulation, then it decreased with time. The decrease in CO<sub>2</sub> concentration was explained by the vertical mixing in the growing boundary layer. The humidity mixing ratio increased at the same time because energy (from the net radiation) was available for evaporation. The LI-7500 humidity time series clearly shows the increase with time of both the amplitude of fluctuations and the size of eddies. The time series of the CO<sub>2</sub> and H<sub>2</sub>O mixing ratios measured by the LI-6262 closed-path analyser connected to MEDEE reproduced the slow variations of the 0.1 s open-path time series well. In contrast, the high frequency variations were not reproduced since the same air sample was analyzed for 11.5 s. The vertical winds corresponding to the times at which the samples were captured are indicated by the red dots on the figure: the value of  $w$  for each dot was computed as the average of the 0.1 s values during the period of the capture.

The second part of Fig. 6 displays a zoom on a 2-min period of the 30-min time series. The two circuits of MEDEE are discriminated with the red and blue colors, on the  $w$  time series (capture dots) and on the closed-path analyser signal (only the CO<sub>2</sub> values are represented here). The central times of the captures are indicated by the vertical dotted lines. The colored CO<sub>2</sub> values are those chosen for DEC flux computation. As indicated above, low-pressure prevented contamination by the previous sample. Using the approach of Langford et al. (2009), the bias due to sample carry-over was estimated on one day of measurement. The average bias was 2.5 % ( $\pm 2$  % standard deviation) for CO<sub>2</sub> fluxes and 2 % ( $\pm 1$  % s.d.) for latent heat fluxes. The amplitudes of concentration variations were well reproduced by the open-path and closed-path analysers; for example, the abrupt  $\sim 20$  ppm decrease observed at 27 min 26 s by the LI-7500 was seen by the LI-6262 but only once a capture (red dot) had been obtained after the decrease.

In the following sections, the EC fluxes of CO<sub>2</sub> and H<sub>2</sub>O are used as the reference for evaluating the DEC fluxes. The EC fluxes were calculated from the 0.1 s time series as described in Sect. 1. In a first step, EC fluxes are compared to simulated DEC (SDEC) fluxes. SDEC time series are defined as a sub-sample of the 0.1 s time series, at a time interval equal to that of the MEDEE system (11.5 s), and with "capture" averaging corresponding to the effective response of the solenoid valves, i.e. the vertical wind as well as the H<sub>2</sub>O and CO<sub>2</sub> time series are averaged on 2–3 consecutive values. The covariances are then computed identically for the complete (10 Hz) and sub-sampled time series. This step must be regarded as a theoretical evaluation of the DEC system, aimed at validating critical parameters like the time interval between the captures and the duration of the capture. In a second step, EC fluxes are compared to DEC fluxes computed from the concentrations measured through MEDEE. In this case, the vertical wind is the only common element between the two systems, and the performance of the DEC prototype can thus be evaluated objectively. No stationarity

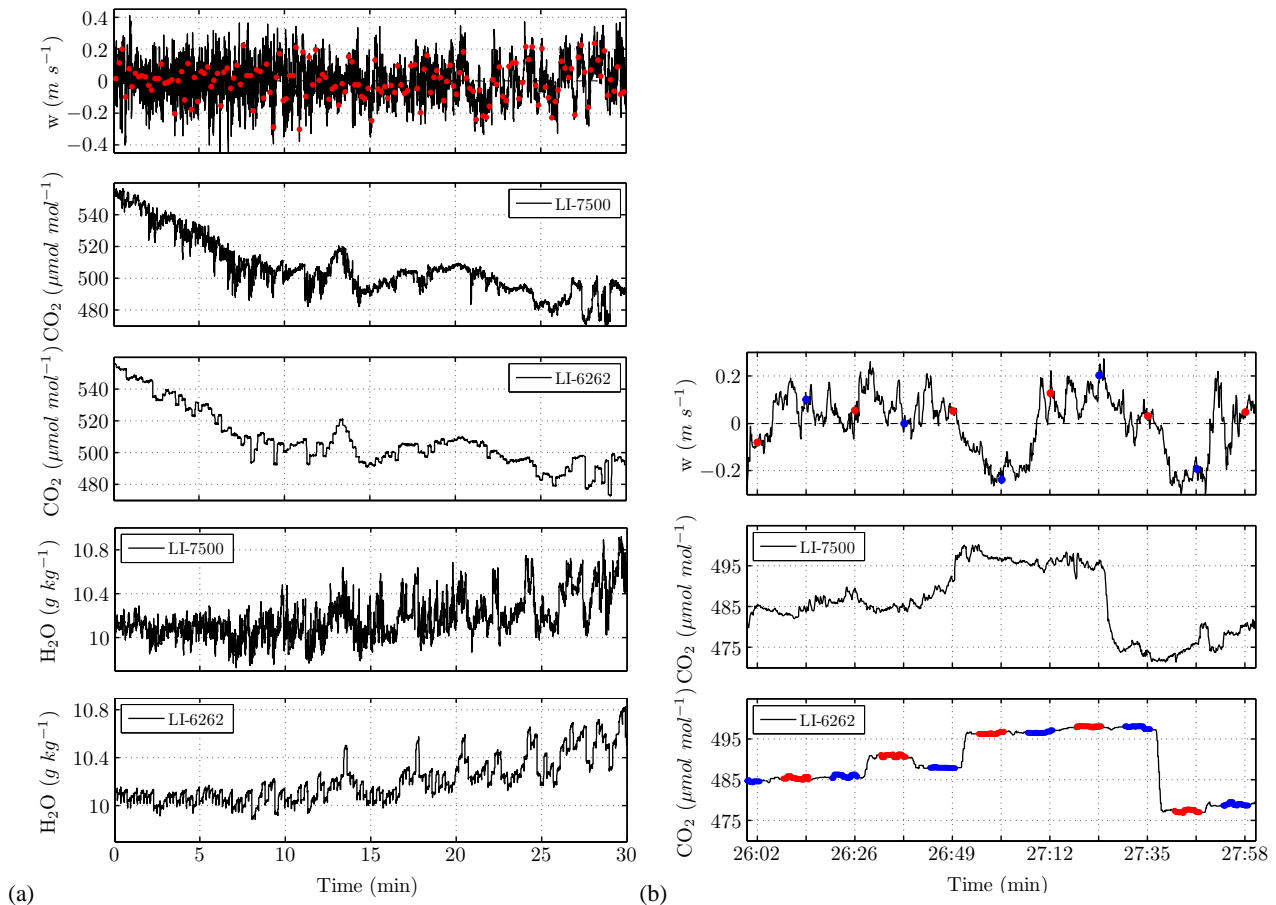


**Fig. 6.** (a) From top to bottom: 30-min time series of  $w$  (m s<sup>-1</sup>), open-path analyser CO<sub>2</sub> mixing ratio (μmol mol<sup>-1</sup>), closed-path analyser CO<sub>2</sub> mixing ratio (μmol mol<sup>-1</sup>), open-path analyser H<sub>2</sub>O mixing ratio (g kg<sup>-1</sup>) and closed-path analyser H<sub>2</sub>O mixing ratio (g kg<sup>-1</sup>). Red dots are  $w$ -values averaged during the captures. (b) Same as above, but restricted to a 2-min period, and without the H<sub>2</sub>O signals. The colored dots on the CO<sub>2</sub> closed path measurements represent the data points used for mixing ratio estimates. The vertical dotted lines represent the sampling times, and the blue and red colors refer to the two reservoirs.

criteria were used to evaluate the flux measurements as the main goal of this study was to compare two techniques with less importance attached to the physical meaning of the measurements.

#### 4.5 Simulated disjunct eddy covariance – eddy covariance inter-comparison

The diurnal course of EC and SDEC fluxes is presented in Fig. 7 for the 15 June case. The weak amplitude of the fluxes is noteworthy. The latent heat flux does not exceed 110 W m<sup>-2</sup> in the middle of the day. Such values are 3–4 times lower than what could be observed above this kind of vegetation but in an active phase (spring). Similarly, CO<sub>2</sub> fluxes do not reach noteworthy values nor do they exhibit a clear diurnal cycle, expressing the absence of photosynthetic activity of the wheat in its ripening phase. On the same site with similar vegetation type, Béziat et al. (2009) reported large changes in net CO<sub>2</sub> as-

simulation, respiration and daily gross ecosystem production (GEP) throughout the season (see their Fig. 4). In April and May, for example, GEP reached daily values of –10 to –15 gC m<sup>-2</sup> day<sup>-1</sup> (1 μmol m<sup>-2</sup> s<sup>-1</sup> ≈ 1.04 gC m<sup>-2</sup> day<sup>-1</sup>). From these daily means, we could expect higher values (i.e. –30 to –45 gC m<sup>-2</sup> day<sup>-1</sup>) in the middle of the day. Despite the low values of the fluxes measured during the validation campaign, the diurnal courses given by the two methods agree in general, though occasional discrepancies are present, which are larger (in relative value) for the CO<sub>2</sub> flux than for the latent heat flux.

The comparison for the whole campaign is presented in Fig. 8 through scatter diagrams. The results are very good for the latent heat flux, with a determination coefficient  $R^2$  of 0.93. Slope and offset of linear regression analysis for Fig. 8b were  $0.99 \pm 0.02$  and  $-0.32 \pm 0.85$  W m<sup>-2</sup>, respectively with standard errors. There is therefore no bias between the two techniques, which demonstrates that the capture time is short enough and turbulent fluctuations are not

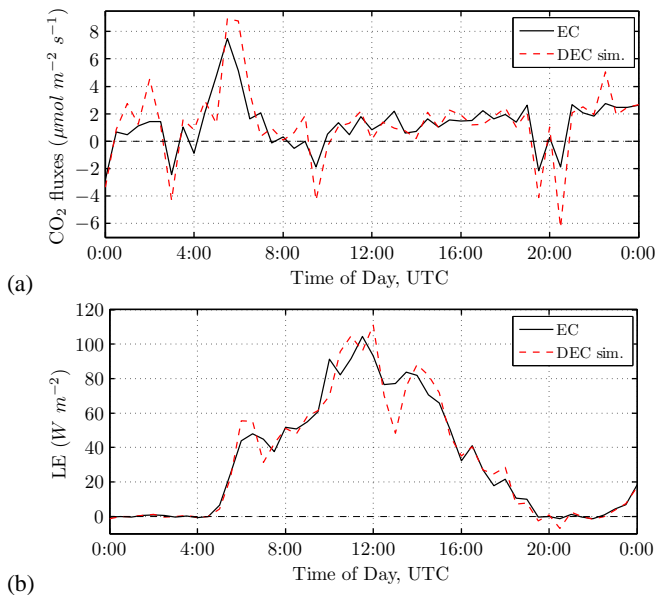


**Fig. 7.** (a) Diurnal course of CO<sub>2</sub> flux ( $\mu\text{mol m}^{-2} \text{s}^{-1}$ ) and (b) latent heat flux ( $\text{W m}^{-2}$ ) measured on 15 June by eddy covariance (solid line) and simulated disjunct eddy covariance (red dashed line) methods.

significantly damped. The scatter is small; the difference between the two methods is not larger than the random error for EC estimates (see, e.g., Lambert and Durand, 1998). The CO<sub>2</sub> flux has larger scatter ( $R^2 = 0.69$ ), which is possibly due to the weakness of the flux. Slope and offset for Fig. 8a were  $1.01 \pm 0.04$  and  $-0.16 \pm 0.08 \mu\text{mol m}^{-2} \text{s}^{-1}$ , respectively. The result of the linear regression analysis shows that despite a significant scatter the two techniques are in agreement for CO<sub>2</sub> fluxes as well. In such conditions, the turbulent part of the concentration signal is reduced with respect to larger scale variations, and the integral scale of the  $w'c'$  time series is increased accordingly, which degrades the performance of both the DEC and EC methods (Lenschow et al., 1994).

#### 4.6 Disjunct eddy covariance – eddy covariance inter-comparison

The EC and DEC fluxes were compared in the same way as for the EC and SDEC fluxes. Figure 9 presents the diurnal course on 15 June. The evolution of the latent heat flux is well reproduced by the two methods, whereas the weakness and small evolution of the CO<sub>2</sub> flux give rise to some discrepancies on a few estimates. It is interesting to note that the observed significant differences on the CO<sub>2</sub> flux occur at the same time and are of the same order as for the EC-SDEC comparison (see Fig. 7). That means that the CO<sub>2</sub> variations observed by the open-path and closed-path analysers are very similar, and that the discrepancies between the fluxes cannot

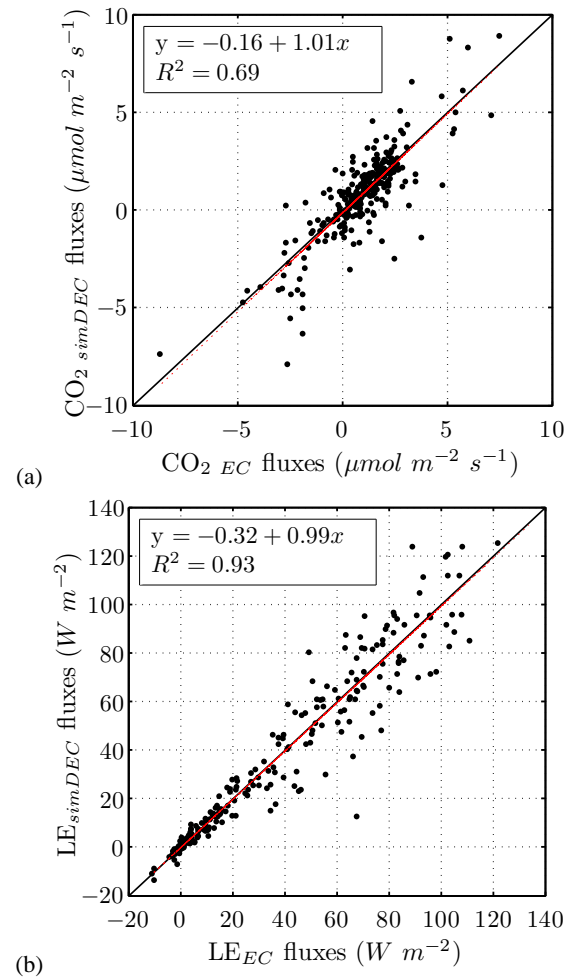


**Fig. 8.** (a) Eddy covariance vs. simulated disjunct eddy covariance CO<sub>2</sub> fluxes ( $\mu\text{mol m}^{-2} \text{s}^{-1}$ ) and (b) latent heat ( $\text{W m}^{-2}$ ). Both graphs report data from the entire field campaign (i.e. from 9 June to 17 June 2011). Solid line is the 1 : 1 line and red dashed line is the linear regression.

be attributed to the MEDEE system but are related to the behavior of the DEC method itself in such conditions.

The comparison for the whole campaign is given in Fig. 10. Determination coefficients  $R^2$  of 0.69 and 0.91 were computed for CO<sub>2</sub> and latent heat fluxes, respectively. Linear regression analysis slope and offset were  $0.86 \pm 0.04$  and  $-0.28 \pm 0.07 \mu\text{mol m}^{-2} \text{s}^{-1}$ , respectively, for CO<sub>2</sub> fluxes. For latent heat fluxes, the slope was  $0.86 \pm 0.02$  and the offset was  $-1.19 \pm 0.80 \text{W m}^{-2}$ . We note that the determination coefficients are very similar to those obtained in the EC-SDEC comparison (see Fig. 8), although the two methods were based on different analysers (open-path for SDEC and closed-path for DEC).

The linear regression analysis showed a similar slope of 0.86 for both CO<sub>2</sub> and latent heat fluxes. Offsets were close to zero in both cases. The linear regression slope indicated

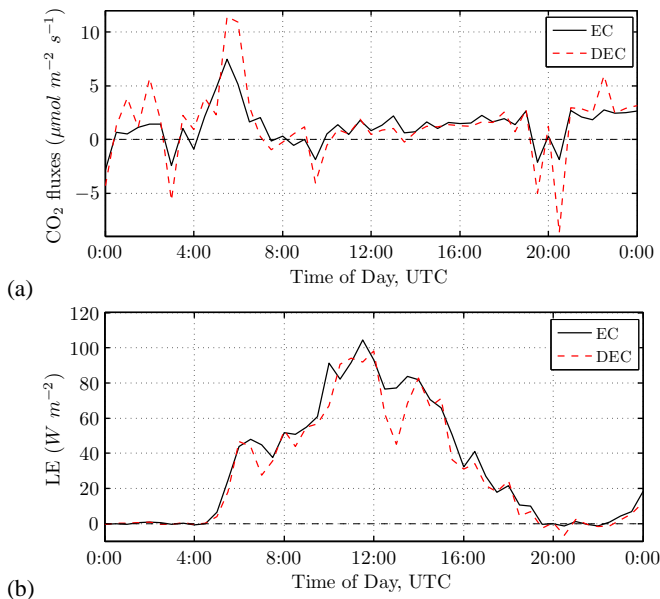


**Fig. 9.** Same as Fig. 7, but for “real” DEC instead of simulated DEC fluxes.

an underestimation of 14 % on DEC fluxes measured by the MEDEE system. This underestimation could come from the sampling system itself or could be due to the sensitivity of the analyser. Additional measurements in higher fluxes conditions are needed to conclude on the origin of this effect. An attenuation of water vapor fluctuations due to surface passivation effects (Lenschow and Raupach, 1991; Massman and Ibrom, 2008) can lead to an underestimation of latent heat fluxes but is not thought to occur significantly here since both CO<sub>2</sub> and latent heat fluxes are identically underestimated.

We should bear in mind that the H<sub>2</sub>O and CO<sub>2</sub> fluxes were weak during the campaign. Higher correlations between EC and DEC fluxes can thus be expected for higher flux conditions.

## 5 BVOC measurements

### 5.1 Site description

The first field campaign for measuring BVOC emissions with MEDEE was carried out at the Oak Observatory at “Observatoire de Haute-Provence” (O3HP) site from 24 July to 6 August 2010. The site is located in the south-east of France, 70 km north of Marseilles, and its vegetation is a forest of 90 % downy oak (*Quercus pubescens*) and 10 % Montpellier maple (*Acer monspessulanum*), with large patches of smoke tree (*Cotinus coggygria*) as undergrowth vegetation. Downy oak is a major tree species in the Mediterranean region and is known to be a strong isoprene emitter (Keenan et al., 2009). In this forest, the trees are about 70 yr old, with a small younger plot located west of the measurement

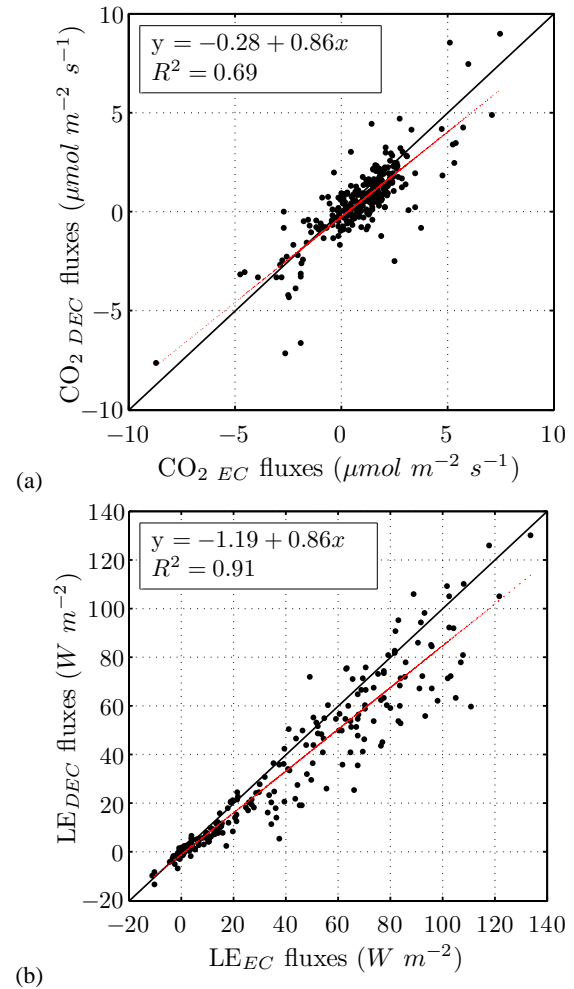


**Fig. 10.** Same as Fig. 8, but for “real” DEC instead of simulated DEC fluxes.

site. The main wind direction is from the north-west (Mistral wind) and the terrain presents a 2 % slope in this direction. The climate is Mediterranean with a dry season somewhat shortened due to the altitude (680 m a.s.l.). The temperature during the measurement period varied between 15 °C at night and 25 °C in the daytime. An 8-m scaffolding tower was set up in the forest with the fast sensors installed above the upper platform at 10 m above the ground (4.5 m above the top of the canopy). Among the sensors, a 3-D sonic anemometer (CSAT 3, Campbell scientific) and a LI-7500 (LI-COR) measured the three wind components, the sonic temperature and the CO<sub>2</sub> and H<sub>2</sub>O concentrations. The MEDEE system was installed on the highest platform of the tower with sample inlets 20 cm away from the sonic transducers. Isoprene concentration was measured with a Fast Isoprene Sensor (Hills Scientific, CO) (Guenther and Hills, 1998), with 4 L min<sup>-1</sup> flow rate coupled to MEDEE. The scaffolding tower was also equipped with radiometers (incoming photosynthetically active radiation (PAR) measured by a LI-190SA (LI-COR),

incoming and outgoing short- and long-wave radiation measured by a Kipp and Zonen CNR1). Ozone and NO<sub>x</sub> analysers were installed in a small cabin 30 m away from the tower with inlets 7 m above ground. The leaf area index (LAI) for the area surrounding the site was measured during the month of August 2010 as part of the O3HP monitoring activity, and was found to be 2.5.

## 5.2 Results and discussion

DEC isoprene flux measurements were performed as well as EC CO<sub>2</sub> and H<sub>2</sub>O fluxes during the measurement period. EC flux calculations were similar to those described in Sect. 4.1 and DEC data were processed as described in Sects. 4.2 and 4.3. The “sonic” temperature was converted into air temperature  $T$  by correcting for moisture contamination, and the sensible heat flux (in  $\text{W m}^{-2}$ ) was computed as the kinematic heat flux ( $\overline{w'T'}$ ) multiplied by  $\rho_a C_p$ , where  $C_p$  is the heat capacity of air at constant pressure. Figure 11 presents the 30-min time series of EC sensible heat flux, CO<sub>2</sub> flux and latent heat flux, and DEC isoprene flux, for 5 and 6 August. 5 August was characterized by a moderate mistral wind with a diurnal average wind speed of  $5.4 \text{ m s}^{-1}$ . Because of the wind, temperatures did not rise above  $22^\circ\text{C}$  for that day. The mistral wind was still present on 6 August but with a lower average wind speed of  $3.3 \text{ m s}^{-1}$ . Maximum temperature for 6 August was  $25^\circ\text{C}$ . The conditions were characteristic of a dry sunny period, with the sensible heat flux reaching 3–4 times the values of the latent heat flux during the day. As expected, the CO<sub>2</sub> uptake occurred during the day due to vegetation photo-synthesis, whereas it reversed during the night due to respiration.

A clear diurnal isoprene emission cycle was observed with values in the range  $1.5\text{--}2.8 \mu\text{g m}^{-2} \text{ s}^{-1}$  around midday. In order to compare these results with previous observations made on the same kind of vegetation, the isoprene fluxes were then normalized to standard conditions (temperature of  $30^\circ\text{C}$  and PAR of  $1000 \mu\text{mol m}^{-2} \text{ s}^{-1}$ ) using the G93 algorithm for isoprene (Guenther et al., 1993; Guenther, 1997). The air temperature measured on the scaffolding tower was used for the conversion instead of leaf temperature because the latter was not available. However, using the surface layer flux-profile relationships to estimate the temperature profile revealed that the day time mean temperature at the top of the canopy did not differ from the air temperature on the scaffolding tower by more than  $1^\circ\text{C}$ . The wind conditions probably explained this small difference, and allowed us to use this temperature as an acceptable approximation to the leaf temperature. The effect of a small underestimation of leaf temperature was estimated to be an increase of a few percent in the averaged normalized flux. Above-canopy PAR was used to normalize isoprene fluxes. This was also a source of error as leaves in the canopy are not evenly exposed to incoming PAR. Isoprene emissions are strongly dependent on PAR at low light level but, beyond 50 % of full sunlight, sat-

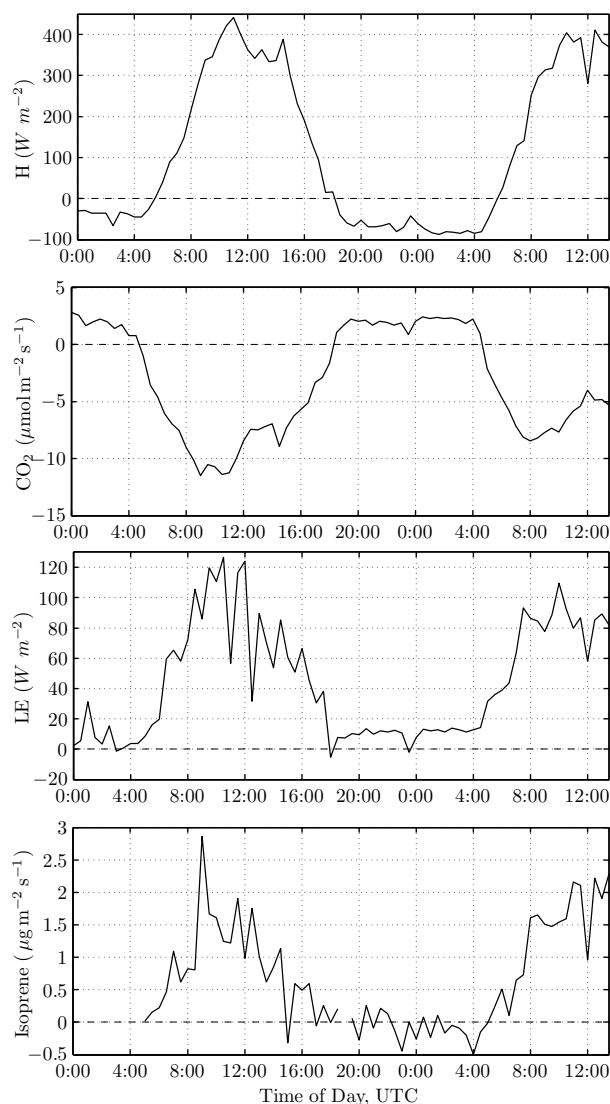


**Fig. 11.** From top to bottom: sensible heat flux ( $\text{W m}^{-2}$ ), CO<sub>2</sub> flux ( $\mu\text{mol m}^{-2} \text{ s}^{-1}$ ) and latent heat flux ( $\text{W m}^{-2}$ ) measured with the eddy covariance method, and Isoprene flux ( $\mu\text{g m}^{-2} \text{ s}^{-1}$ ) computed with the disjunct eddy covariance method. The measurement period was on 5 and 6 August 2010.

uration occurs (Guenther et al., 1993). The effect of using overestimated PAR values to normalize emission rates was estimated by calculating the normalized fluxes with PAR values reduced by 50 %. The result showed that using above canopy PAR leads to a 7 % decrease in the averaged normalized flux. Considering a LAI value of 2.5 on this field site, the average PAR for the whole canopy is expected to be higher than 50 % of the above canopy value. The normalized fluxes were then converted into standard emission rates, using the measured LAI on the site and a leaf mass per area value of  $134.3 \text{ g m}^{-2}$  given by Simon et al. (2005) for a downy oak forest in the same area and presenting very

similar morphology. Isoprene standard emission rates were averaged from 07:00 to 14:00 UTC for the two days. The resulting standard emission rate was 40  $\mu\text{g g}^{-1} \text{h}^{-1}$ . Simon et al. (2005), Owen et al. (1998), Steinbrecher et al. (1997) and Kesselmeier et al. (1998) report isoprene standard emission rates of 134.7, 92, 90.7 and 42  $\mu\text{g g}^{-1} \text{h}^{-1}$ , respectively, for *Quercus Pubescens*. In these studies, measurements were performed using branch enclosures. Above-canopy flux can be expected to be lower than branch-level flux because of removal processes that can occur, such as surface deposition in the canopy or chemical transformation of isoprene between the leaf and the above-canopy areas (Fuentes et al., 2000). The windy conditions can also have a lowering effect on emission rates (Loreto and Sharkey, 1993). The value found in the present study, although in the lower range, compares reasonably well with the values reported in the literature considering the measurement technique that was used.

## 6 Conclusions

The goal of this study was to develop, validate, and deploy a new DEC flux measurement system called MEDEE. This system was made of chemically inert materials to avoid sample contamination and built to meet aircraft (the French ATR-42 in a first step) requirements. The MEDEE system is able to quickly take 1 L air samples and ensure their continuous transfer at constant pressure to an online analyser. The system is built as twin mechanical syringes, whose alternate functioning ensures a continuous supply to the on-line analyser. MEDEE was operated with a switching period from one sample to the other of 11.5 s, which fulfils the requirements for keeping good accuracy on the covariance estimate in spite of the reduced number of data. With such intervals and the reservoir volume, the system can be connected to on-line analysers with flow rates of up to 4 L  $\text{min}^{-1}$ . The stability of the pressure (of the order of 1–2 hPa) favours better functioning of most analysers. These features make MEDEE suitable for measurements of different trace gases and compatible with a wide array of analysers. For example, the quantum cascade laser absorption spectrometer (QCLAS) (Joly et al., 2011) or the cavity ringdown spectrometer (CDRS) (Crosson, 2008; Langridge et al., 2008; Fiddler et al., 2009), which monitor trace gases such as CO, CH<sub>4</sub>, N<sub>2</sub>O or NO<sub>x</sub>.

The system was validated through a field campaign during which H<sub>2</sub>O and CO<sub>2</sub> fluxes were simultaneously measured with EC and DEC techniques with different analysers. The EC fluxes were used as a reference. In a first step, which can be considered as a theoretical validation, the EC fluxes were compared to the simulated DEC fluxes calculated from the sub-sampled high-rate time series, but taking the averaging resulting from non-instantaneous filling time into account. Despite the weak CO<sub>2</sub> and latent heat fluxes observed during the campaign, good correlation was found between the two methods with determination coefficients  $R^2$  of 0.93 and

0.69 for H<sub>2</sub>O and CO<sub>2</sub> fluxes, respectively. The comparison between EC and “real” DEC fluxes provided very similar  $R^2$  coefficients, however a 14 % underestimation of DEC fluxes was observed on linear regression analyses for both CO<sub>2</sub> and Latent heat fluxes. Further experiments need to be conducted in higher flux conditions to determine the reason for this effect.

MEDEE was also tested for BVOC flux measurements over a downy oak forest. The results showed a standard (30 °C, 1000  $\mu\text{mol m}^{-2} \text{s}^{-1}$ ) isoprene emission rate of 40  $\mu\text{g g}^{-1} \text{h}^{-1}$ , in the lower range of values reported in the literature for comparable vegetation. Such measurements will be made in the coming years in the framework of the Chemistry-Aerosol Mediterranean Experiment (ChArMEX) project, in order to improve the parameterization of the BVOC emission rates. It is planned to improve the parameterization of the emission by taking parameters other than the PAR and temperature into account.

MEDEE is also scheduled for airborne measurements on the French ATR-42 aircraft. This aircraft is equipped for turbulence measurements (Saïd et al., 2010) and the use of MEDEE with a PTR-MS will allow the estimation of BVOC fluxes at landscape scale and throughout the atmospheric boundary layer.

*Acknowledgements.* We would like to express our gratitude to Romain Mathon and Driss Kouach from the Groupe Instrumentation Scientifique at OMP, and to Jean-Michel Martin, Lei Liu and Guillaume Sokolof who did great work and provided support for the realization of MEDEE. Our recognition also goes to the OHP and CESBIO teams, especially to Thierry Gauquelin, Michel Boer, Ilja Reiter, Jean-Philippe Orts, Bernard Marciel and Hervé Gibrin for their help during the field campaign. Valuable comments on the manuscript by Jean-Luc Attié and Eric Ceschia were much appreciated. This work was supported by INSU/CNRS (through the LEFE-CHAT and MISTRALS programmes), the Observatoire Midi-Pyrénées and the Laboratoire d’Aérodologie.

Edited by: C. Ammann



The publication of this article is financed by CNRS-INSU.

## References

- Andreas, E. L., Hill, R. J., Gosz, J. R., Moore, D. I., Otto, W. D., and Sarma, A. D.: Stability dependence of the eddy accumulation coefficients for momentum and scalars, *Bound.-Lay. Meteorol.*, 86, 409–420, 1998.
- Aubinet, M., Grelle, A., Ibrom, A., Rannik, Ü., Moncrieff, J., Foken, T., Kowalski, A. S., Martin, P. H., Berbigier, P., Bernhofer, C., Clement, R., Elbers, J., Granier, A., Grünwald, T., Morgenstern, K., Pilegaard, K., Rebmann, C., Snijders, W., Valentini, R., and Vesala, T.: Estimates of the Annual Net Carbon and Water Exchange of Forests: The EUROFLUX Methodology, *Adv. Ecol. Res.*, 30, 113–175, 1999.
- Baldocchi, D. D., Hincks, B. B., and Meyers, T. P.: Measuring Biosphere-Atmosphere Exchanges of Biologically Related Gases with Micrometeorological Methods, *Ecology*, 69, 1331–1340, 1988.
- Béziat, P., Ceschia, E., and Dedieu, G.: Carbon balance of a three crop succession over two cropland sites in South West France, *Agr. Forest Meteorol.*, 149, 1628–1645, 2009.
- Blake, R. S., Monks, P. S., and Ellis, A. M.: Proton-Transfer Reaction Mass Spectrometry, *Chem. Rev.*, 109, 861–896, doi:10.1021/cr800364q, 2011.
- Businger, J. A. and Oncley, S. P.: Flux Measurement with Conditional Sampling, *J. Atmos. Oceanic Technol.*, 7, 349–352, 1990.
- Crosson, E. R.: A cavity ring-down analyzer for measuring atmospheric levels of methane, carbon dioxide, and water vapour, *Appl. Phys. B-Lasers O.*, 92, 403–408, 2008.
- Dabberdt, W. F., Lenschow, D. H., Horst, T. W., Zimmerman, P. R., Oncley, S. P., and Delany, A. C.: Atmosphere-Surface Exchange Measurements, *Science*, 260, 1472–1481, 1993.
- Desjardins, R. L.: Description and evaluation of a sensible heat flux detector, *Bound.-Lay. Meteorol.*, 11, 147–154, 1977.
- Dolman, A. J., Noilhan, J., Durand, P., Sarrat, C., Brut, A., Pignatelli, B., Butet, A., Jarosz, N., Brunet, Y., Loustau, D., Lamaud, E., Tolk, L., Ronda, R., Miglietta, F., Gioli, B., Magliulo, V., Esposito, M., Gerbig, C., Körner, S., Glademard, P., Ramonet, M., Ciais, P., Neininger, B., Hutjes, R. W. A., Elbers, J. A., Macatangay, R., Schrems, O., Pérez-Landa, G., Sanz, M. J., Scholz, Y., Facon, G., Ceschia, E., and Béziat, P.: The CarboEurope Regional Experiment Strategy, *B. Am. Meteorol. Soc.*, 87, 1367–1379, 2006.
- Fiddler, M. N., Begashaw, I., Mickens, M. A., Collingwood, M. S., Assefa, Z., and Bililign, S.: Laser Spectroscopy for Atmospheric and Environmental Sensing, *Sensors*, 9, 10447–10512, 2009.
- Foken, T. and Wichura, B.: Tools for quality assessment of surface-based flux measurements, *Agr. Forest Meteorol.*, 78, 83–105, 1996.
- Fotiadi, A. K., Lohou, F., Druilhet, A., Serça, D., Saïd, F., Laville, P., and Brut, A.: Methodological Development on the Conditional Sampling Method Part I: Sensitivity to Statistical and Technical Characteristics, *Bound.-Lay. Meteorol.*, 114, 615–640, 2005.
- Fuehrer, P. L. and Friehe, C. A.: Flux correction revised, *Bound.-Lay. Meteorol.*, 102, 415–457, 2002.
- Fuentes, J. D., Lerdau, M., Atkinson, R., Baldocchi, D., Bottenheim, J. W., Ciccioli, P., Lamb, B., Geron, C., Gu, L., Guenther, A., Sharkey, T. D., and Stockwell, W.: Biogenic hydrocarbons in the atmospheric boundary layer: a review, *B. Am. Meteorol. Soc.*, 81, 1537–1575, 2000.
- Grabner, W., Graus, M., Lindinger, C., Wisthaler, A., Rappenglück, B., Steinbrecher, R., and Hansel, A.: Disjunct eddy covariance measurements of monoterpene fluxes from a Norway spruce forest using PTR-MS, *Int. J. Mass Spectrom.*, 239, 111–115, 2004.
- Guenther, A.: Seasonal and Spatial Variations in Natural Volatile Organic Compound Emissions, *Ecol. Appl.*, 7, 34–45, 1997.
- Guenther, A. B. and Hills, A. J.: Eddy covariance measurement of isoprene fluxes, *J. Geophys. Res.*, 103, 13145–13152, 1998.
- Guenther, A. B., Zimmerman, P. R., Harley, P. C., Monson, R. K., and Fall, R.: Isoprene and Monoterpene Emission Rate Variability: Model Evaluations and Sensitivity Analyses, *J. Geophys. Res.*, 98, 12609–12617, 1993.
- Joly, L., Zéninari, V., Decarpenterie, T., Cousin, J., Grouiez, B., Mammez, D., Durry, G., Carras, M., Marcadet, X., and Parvitte, B.: Continuous-wave quantum cascade lasers absorption spectrometers for trace gas detection in the atmosphere, *Laser Phys.*, 21, 805–812, 2011.
- Karl, T. G., Spirig, C., Rinne, J., Stroud, C., Prevost, P., Greenberg, J., Fall, R., and Guenther, A.: Virtual disjunct eddy covariance measurements of organic compound fluxes from a subalpine forest using proton transfer reaction mass spectrometry, *Atmos. Chem. Phys.*, 2, 279–291, doi:10.5194/acp-2-279-2002, 2002.
- Keenan, T., Niinemets, Ü., Sabate, S., Gracia, C., and Peñuelas, J.: Process based inventory of isoprenoid emissions from European forests: model comparisons, current knowledge and uncertainties, *Atmos. Chem. Phys.*, 9, 4053–4076, doi:10.5194/acp-9-4053-2009, 2009.
- Kesselmeier, J., Bode, K., Schäfer, L., Schebeske, G., Wolf, A., Brancaleoni, E., Cecinato, A., Ciccioli, P., Frattoni, M., Dutaur, L., Fugit, J. L., Simon, V., and Torres, L.: Simultaneous field measurements of terpene and isoprene emissions from two dominant mediterranean oak species in relation to a North American species, *Atmos. Environ.*, 32, 1947–1953, 1998.
- Kristensen, L., Lenschow, D. H., Gurarie, D., and Jensen, N. O.: A simple model for the vertical transport of reactive species in the convective atmospheric boundary layer, *Bound.-Lay. Meteorol.*, 134, 195–221, 2009.
- Lambert, D. and Durand, P.: Aircraft-to-aircraft intercomparison during SEMA-PHORE, *J. Geophys. Res.*, 103, 25109–25123, 1998.
- Langford, B., Davison, B., Nemitz, E., and Hewitt, C. N.: Mixing ratios and eddy covariance flux measurements of volatile organic compounds from an urban canopy (Manchester, UK), *Atmos. Chem. Phys.*, 9, 1971–1987, doi:10.5194/acp-9-1971-2009, 2009.
- Langridge, J. M., Laurila, T., Watt, R. S., Jones, R. L., Kaminski, C. F., and Hult, J.: Cavity enhanced absorption spectroscopy of multiple trace gas species using a supercontinuum radiation source, *Opt. Express*, 16, 10178–10188, 2008.
- Lee, X. and Massman, W.: A perspective on thirty years of the Webb, Pearman and Leuning density corrections, *Bound.-Lay. Meteorol.*, 139, 37–59, 2011.
- Lenschow, D. H. and Raupach, M. R.: The Attenuation of Fluctuations in Scalar Concentrations through Sampling Tubes, *J. Geophys. Res.*, 96, 15259–15268, doi:10.1029/91JD01437, 1991.
- Lenschow, D. H., Mann, J., and Kristensen, L.: How Long Is Long Enough When Measuring Fluxes and Other Turbulence Statistics?, *J. Atmos. Ocean.-Tech.*, 11, 661–673, 1994.

- Lohou, F., Saïd, F., Lothon, M., Durand, P. and Serça, D.: Impact of Boundary-Layer Processes on Near-Surface Turbulence Within the West African Monsoon, *Bound.-Lay. Meteorol.*, 136, 1–23, doi:10.1007/s10546-010-9493-0, 2010.
- Loreto, F. and Sharkey, T. D.: Isoprene emission by plants is affected by transmissible wound signals, *Plant Cell Environ.*, 16, 563–570, 1993.
- Massman, W. J. and Ibrom, A.: Attenuation of concentration fluctuations of water vapor and other trace gases in turbulent tube flow, *Atmos. Chem. Phys.*, 8, 6245–6259, doi:10.5194/acp-8-6245-2008, 2008.
- Moore, C. J.: Frequency response corrections for eddy correlation systems, *Bound.-Lay. Meteorol.*, 37, 17–35, 1986.
- Owen, S. M., Boissard, C., Hagenlocher, B., and Hewitt, C. N.: Field studies of isoprene emissions from vegetation in the North-west Mediterranean region, *J. Geophys. Res.*, 103, 25499–25511, 1998.
- Pielke, R. A., Avissar Sr., R., Raupach, M., Dolman, A. J., Zeng, X., and Denning, A. S.: Interactions between the atmosphere and terrestrial ecosystems: influence on weather and climate, *Global Change Biol.*, 4, 461–475, 1998.
- Rinne, J. and Ammann, C.: Disjunct Eddy Covariance Method, in: *Eddy Covariance*, edited by: Aubinet, M., Vesala, T., and Papale, Springer, ISBN 978-94-007-2350-4, 289–305, 2012.
- Rinne, J., Delany, A., Greenberg, J., and Guenther, A.: A true eddy accumulation system for trace gas fluxes using disjunct eddy sampling method, *J. Geophys. Res.*, 105, 24791–24798, 2000.
- Rinne, J., Guenther, A., Warneke, C., de Gouw, J., and Luxembourg, S.: Disjunct eddy covariance technique for trace gas flux measurements, *Geophys. Res. Lett.*, 28, 3139–3142, 2001.
- Rinne, J., Durand, P., and Guenther, A.: An airborne disjunct eddy covariance system: Sampling strategy and instrument design, *Proc. 15th Symposium on Boundary Layers and Turbulence*, 15–19 July 2002, Wageningen, The Netherlands, AMS Ed., 151–154, 2002.
- Rinne, J., Douffet, T., Prigent, Y., and Durand, P.: Field comparison of disjunct and conventional eddy covariance techniques for trace gas flux measurements, *Environ. Pollut.*, 152, 630–635, 2008.
- Saïd, F., Canut, G., Durand, P., Lohou, F., and Lothon, M.: Seasonal evolution of the boundary-layer turbulence measured by aircraft during AMMA 2006 Special Observation Period, *Q. J. Roy. Meteor. Soc.*, 136, 47–65, 2010.
- Simon, V., Dumergues, L., Bouchou, P., Torres, L., and Lopez, A.: Isoprene emission rates and fluxes measured above a Mediterranean oak (*Quercus pubescens*) forest, *Atmos. Res.*, 74, 49–63, 2005.
- Steinbrecher, R., Hauff, K., Rabong, R., and Steinbrecher, J.: Isoprenoid emission of oak species typical for the Mediterranean area: Source strength and controlling variables, *Atmos. Environ.*, 31, Supplement 1, 79–88, 1997.
- Turnipseed, A. A., Pressley, S. N., Karl, T., Lamb, B., Nemitz, E., Allwine, E., Cooper, W. A., Shertz, S., and Guenther, A. B.: The use of disjunct eddy sampling methods for the determination of ecosystem level fluxes of trace gases, *Atmos. Chem. Phys.*, 9, 981–994, doi:10.5194/acp-9-981-2009, 2009.
- Vilà-Guerau de Arellano, J. and Duynkerke, P. G.: Influence of chemistry on the Flux-Gradient relationships for the NO-O<sub>3</sub>-NO<sub>2</sub> system, *Bound.-Lay. Meteorol.*, 61, 375–387, 1992.
- Webb, E. K., Pearman, G. I., and Leuning, R.: Correction of flux measurements for density effects due to heat and water vapour transfer, *Q. J. Roy. Meteor. Soc.*, 106, 85–100, 1980.